Novel Characterization of Capsule X-Ray Drive at the National Ignition Facility

S. A. MacLaren,[1,*] M. B. Schneider,[1] K. Widmann,[1] J. H. Hammer,[1] B. E. Yoxall,[1] J. D. Moody,[1] P. M. Bell,[1] L. R. Benedetti,[1] D. K. Bradley,[1] M. J. Edwards,[1] T. M. Guymer,[2] D. E. Hinkel,[1] W. W. Hsing,[1] M. L. Kervin,[1] N. B. Meezan,[1] A. S. Moore,[2] and J. E. Ralph[1]

[1]*Lawrence Livermore National Laboratory, P.O. Box 808, Livermore, California 94550, USA*

[2]*Atomic Weapons Establishment, Aldermaston, Reading RG7 4PR, United Kingdom*

(Received 24 September 2013; published 13 March 2014)

Indirect drive experiments at the National Ignition Facility are designed to achieve fusion by imploding a fuel capsule with x rays from a laser-driven hohlraum. Previous experiments have been unable to determine whether a deficit in measured ablator implosion velocity relative to simulations is due to inadequate models of the hohlraum or ablator physics. ViewFactor experiments allow for the first time a direct measure of the x-ray drive from the capsule point of view. The experiments show a 15%–25% deficit relative to simulations and thus explain nearly all of the disagreement with the velocity data. In addition, the data from this open geometry provide much greater constraints on a predictive model of laser-driven hohlraum performance than the nominal ignition target.

DOI: 10.1103/PhysRevLett.112.105003 PACS numbers: 52.50.Jm, 52.70.La

The National Ignition Facility (NIF) [1] at Lawrence Livermore National Laboratory is engaged in the pursuit of fusion ignition using indirect drive [2]. In this technique, up to 1.8 MJ of laser energy is converted to x-ray drive which implodes a capsule consisting of a deuterium-tritium fuel surrounded by a plastic ablator [3]. The conversion occurs in a gas-filled gold hohlraum containing the fuel capsule with laser entrance holes (LEH) at either end. The gold walls absorb and reemit x rays, creating a time-dependent x-ray drive that is absorbed in a thin "ablation" region. The CH in this region ionizes, becomes optically thin to the x-ray drive, and expands radially outward, generating an inward pressure in a "rocket" effect that implodes the capsule [4,5].

Imaging data [4,6] of capsule radius vs time measure a lower velocity than simulated (260 vs 300 km/s for a 1.3 MJ drive), suggesting that either the radiation drive is lower than predicted, or the ablator is less efficient at converting the energy to useful hydrodynamic work than expected, or a combination of both [7]. Implosion data can be matched if the integrated simulations use time-dependent multipliers of about 0.8 at the peak of the laser drive [6]. The current "standard" model for laser hohlraum simulation is the product of decades of development and contains key improvements based on recent NIF data [8]. However, in this Letter the ViewFactor data demonstrate that the cause of the reduced implosion speed is a deficit in x-ray drive relative to simulations. This finding indicates shortcomings in the current modeling of the laser-produced x-ray drive, which was based mostly on measurements of hohlraums and gold spheres in vacuum [8]. The results in this Letter indicate that it is the model for x-ray production in gas filled hohlraums and not ablation physics that must be improved to gain predictive capability for indirect-drive ignition experiments.

The ViewFactor experiment, shown in Fig. 1, employs an ignition-scale cryogenic hohlraum [3] which is truncated on one side 2 mm beyond the hohlraum center, allowing diagnostics to directly view the hohlraum interior and the far LEH for absolute measurements of x-ray flux and x-ray imaging. The purpose of the experiments is to characterize the x-ray drive from the viewpoint of a capsule, as opposed to the usual measurement of the drive through the LEH from which the capsule drive is inferred [5]. The experiments are designed to create a plasma environment as close as possible to the ignition target while allowing for a more complete view of the hohlraum interior. We show that ViewFactor experiments measure lower capsule drive than the LEH-inferred drive and are consistent with slower implosion speeds. The drive deficit of 15%–25% represents almost all of the discrepancy between simulations and the observed implosion hydrodynamics.

The nominal ignition hohlraum is 5.75 mm in diameter, 9.425 mm long, with 3.1 mm LEHs. The ViewFactor target has one half identical to the ignition hohlraum but the other half extends only 2 mm beyond the hohlraum center, with an opening equal to the full diameter of the hohlraum as shown in Fig. 1. The ViewFactor target is shot at cryogenic temperature (32 K) and is filled with He gas at 0.96 mg/cc, the same mass density as in the ignition design. The fuel capsule is replaced by a thin plastic spherical shell (3 mm diameter with 20 or 30 μm shell thickness). The thin shell is almost completely ablated by the peak of the drive.

The experiment was designed so that the plasma conditions at the LEH end at the time of peak drive are matched to those of the ignition hohlraum. This was accomplished by varying the radius and thickness of the capsule in the simulation and comparing the measured backscatter to that of a typical ignition hohlraum. Because of the large open

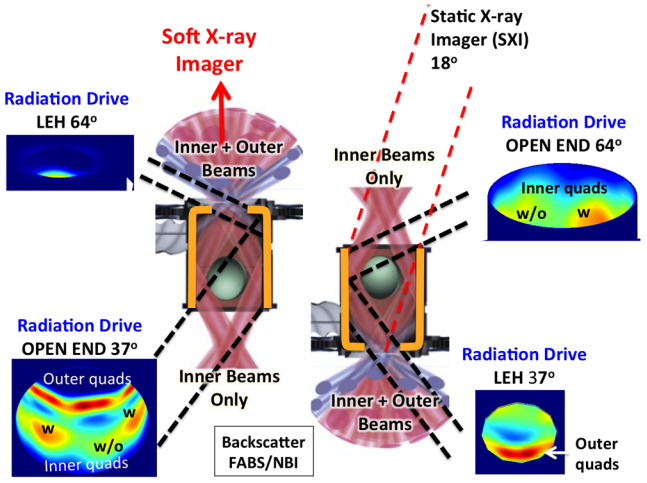

FIG. 1 (color online). The experimental configuration showing the ViewFactor truncated hohlraum and its two orientations, open end down (on left) and open end up (on right). The views from the four radiation drive measurements are also shown. These simulated VISRAD [9] images use a geometry roughly consistent with the positions and intensities of the quads at peak drive; for the two views of the open end, the inner quads are labeled either "w" meaning the quad is from the LEH side and energy is transferred to it, or "w/o" meaning it is from the open end and does not undergo CBET. FABS and NBI diagnostics measure backscatter from both open and LEH ends of the target.

area, the maximum radiation temperature in the simulations was 270 eV for ViewFactor, a drop of 20 eV from the ignition hohlraum. By the time of peak drive, the thin capsule has been mostly ablated and is optically thin, allowing emission from the hohlraum to be measured directly.

The hohlraum is driven with a standard ignition laser pulse shape at the LEH end divided between 32 inner beams at 23.5° and 30° and 64 outer beams at 44.5° and 50°. Because of the truncated geometry, only the inner beams are used at the open end. In an ignition hohlraum, the power balance between inner and outer beams can be adjusted by tuning the laser wavelength difference between them in a process known as cross beam energy transfer (CBET) [10]. Without the outer beams the CBET effect will not be present in the open end; however, to maintain the surrogacy of the LEH end of the ViewFactor target with a typical gas-filled ignition hohlraum, the wavelength difference between the (30°) and outer beams was 7.9 Å and between the (23.5°) beams and outer beams was 9.1 Å. This wavelength shift was made at 1ω before the light is frequency tripled to 351 nm. ViewFactor experiments are done in pairs, with one shot employing the open end down configuration (Fig. 1, left) and the other employing open end up (Fig. 1, right). This allows all diagnostics to record data viewing both the open end and the LEH end.

The hohlraum x-ray emission is measured with the Dante diagnostic [11], a time-resolved, low resolution x-ray spectrometer consisting of 18 channels of filtered x-ray diodes. There are two Dantes in the NIF target chamber, one viewing the target at 37° to its axis in the lower hemisphere, and one viewing the target at 64° to its axis in the upper hemisphere. Figure 1 shows views of the target as seen by both Dantes in both configurations made with the VISRAD code [9]. An LEH diameter of 2.66 mm and a hohlraum diameter of 5.28 mm were used to mimic plasma motion to place the beam spots in roughly their positions at peak drive.

The size of the LEH vs time is measured with a gated, 4-strip microchannel plate detector [12] coupled to a soft x-ray imager snout [13]. The snout consists of two soft channels near 500 and 900 eV and one hard channel > 4 keV. It views down the hohlraum axis from the top of the chamber. The open geometry allows for effective imaging of time-dependent LEH size viewed both internally (open end up) and externally (open end down).

Backscatter measurements [14] consist of a full aperture backscatter system (FABS) made up of diodes, spectrometers, and streak cameras to measure light directly backscattered into the four beams of a 30° and a 50° quad and a near backscatter imager (NBI) to measure light scattered just outside the beam ports for a 23.5° and a 30° quad.

The ViewFactor experiments were modeled with the LASNEX code [15] using the high flux model [8] adopted after the 2009 NIF campaign [16]. It uses a flux limiter based on the Spitzer formula for electron conduction of $f = 0.15$ and it uses the detailed configuration accounting (DCA) NLTE atomic physics model [17] to generate opacities responsible for emission. The simulation is first run using the measured laser energy to establish plasma conditions. The cross beam energy transfer is calculated for these plasma conditions, the laser pulses are modified using this energy transfer and the measured backscatter, and the model is run again [18].

To compare to the data, post shot simulations have been postprocessed to give simulated Dante drive signals and simulated images. Postprocessing the simulations with and without the thin capsule material showed a negligible difference for the 37° drive diagnostic viewing the open end.

Two pairs of ViewFactor shots are discussed. The first pair used a capsule with shell thickness of 20 μm. The backscatter at the LEH end was 11%, indicating the coupling at the LEH end was $89 \pm 2\%$. The shell thickness was increased to 30 μm for the second pair of shots and the coupling at the LEH end was $86 \pm 2\%$. This indicated better surrogacy to plasma conditions in an ignition hohlraum which typically has a coupling of about 84% [7]. Direct comparison of the 30 μm ViewFactor target to a comparable ignition hohlraum reveals both lose most of their backscattered energy to SRS from the inner beams: 11% and 12.6% for the ignition and ViewFactor targets, respectively. Additionally, the time- and spectrally resolved SRS power measurements for the two shots are nearly

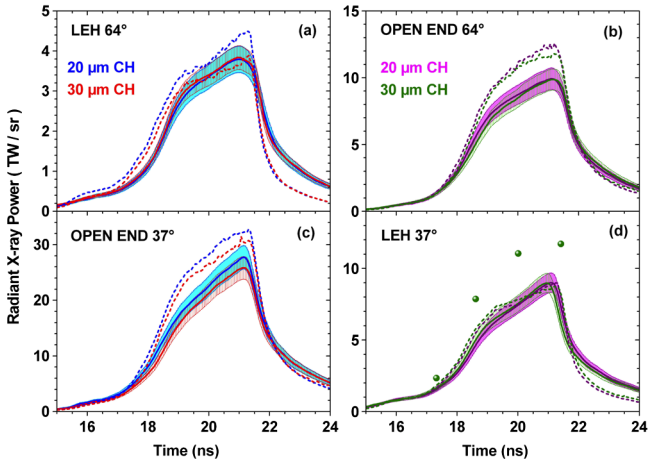

FIG. 2 (color online). Measured and simulated radiant x-ray power vs time from the two Dante views of each of the four shots. Solid lines are measurements with the experimental uncertainties indicated either by the shaded or hatched region; dashed lines are simulated Dante data. The graphs are arranged in the same order as the Dante views shown in Fig. 1: (a) 64° view of the LEH (b) 64° view of the open end (c) 37° view of the open end (d) 37° view of the LEH. Blue and magenta traces are obtained for targets with a 20 μm thick capsule shell, and red and green traces are from shots that employed capsules with a 30 μm thick shell. The green points in (d) are the LEH-view simulation (dashed green curve) corrected for source size using the time-resolved measurements of the LEH size.

identical except for a 10–20 nm shift to smaller wavelength for the ViewFactor.

Figure 2 compares the measured radiant x-ray power for the four views with the simulated power. As Figure 1 indicates, the 37° view of the open end [Fig. 2(c)] offers the most complete view of the hohlraum interior, exposing both inner and outer cone beam spots to the view of the diagnostic. This view emulates the capsule view of the radiation drive and Fig. 2(c) shows the simulation overpredicts it by 20%–25%, but Fig. 2(d) shows that the simulations indicated by the dashed curves are in reasonably good agreement with the 37° LEH view. Time-resolved measurements of the LEH size, described later, were made for the 30 μm ViewFactor target; these may be compared with the simulated LEH size and used to compute a source-size corrected Dante x-ray power history from the simulation shown by the green points in Fig. 2(d). Based on the image analysis, the source size correction to the simulated x-ray power has an error of $\pm 4\%$.

Making use of the solid angles and spectral response of the Dante channels, the simulation results may be forward processed to generate individual channel voltages for comparison with data. This comparison is shown in Fig. 3 for three individual Dante channels from the 37° open end view. For the channel with response in the range of 0.80 to 0.93 keV near the peak of the thermal spectrum emission [Fig. 3(a)], the predicted signal is greater than the data by a similar fraction as for the spectrally integrated flux in Fig. 2(c). For the channel at the x-ray energy of 2.3 to 2.8 keV near the peak of the $4 \rightarrow 3$ M-shell transition array [19] that could preheat the ignition capsule [Fig. 3(b)], the simulation does a good job of reproducing the data. For the channel closest to the SXI hard x-ray range at 3.1 to 4.9 keV [Fig. 3(c)], the simulated voltage peak matches the data, but the simulation exhibits the earlier, steeper rise characteristic of the integrated power measurement.

As mentioned earlier, time dependent multipliers on the laser power are typically necessary for integrated simulations to match the measured implosion performance [6]. Figure 4 plots the time-dependent ratio of the radiant x-ray power of the open end of the ViewFactor target measured by the 37° Dante to that generated by the simulation from Fig. 2(c), together with the multipliers used to modify the laser power for an implosion calculation. Beginning at

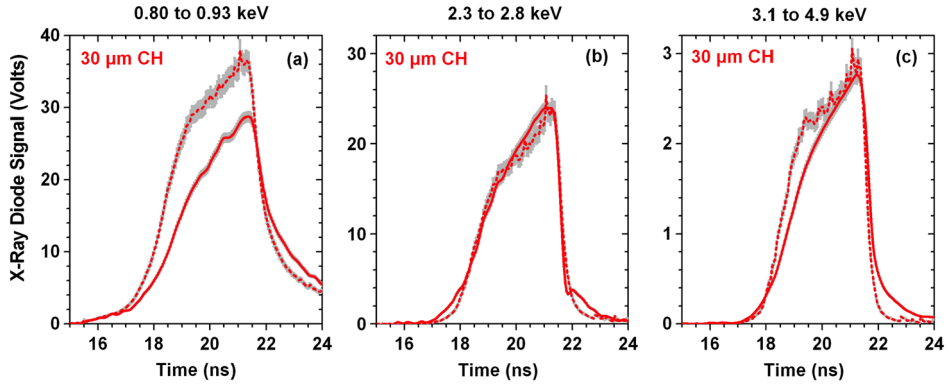

FIG. 3 (color online). Comparison of measured (solid) and simulated (dashed) x-ray diode signals for (a) Cu filtered, (b) Saran filtered, and (c) Ti filtered channels for the open end view at 37° [Fig. 2(c)]. The energy range listed above each plot is the FWHM of the corresponding response functions for these channels. The shaded areas indicate the uncertainties. The error for the measured values indicates the uncertainty in the experimental determination of the x-ray diode signal. The error shown for the simulated values is due to the uncertainties in the response functions for each channel.

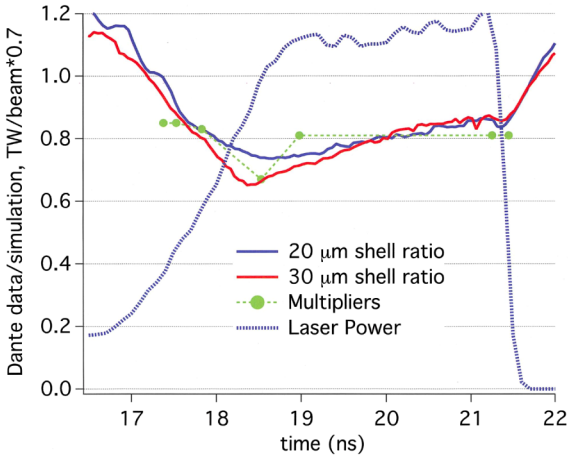

FIG. 4 (color online). The solid red and blue curves represent the ratio of the measured 37° Dante radiant x-ray power (in GW/sr) to the simulated values for the two open-end-down targets. The dashed blue curve is the laser power history (TW/beam) scaled by 0.7. The green points represent the multipliers on the laser power needed for integrated ignition target simulations to match capsule implosion data.

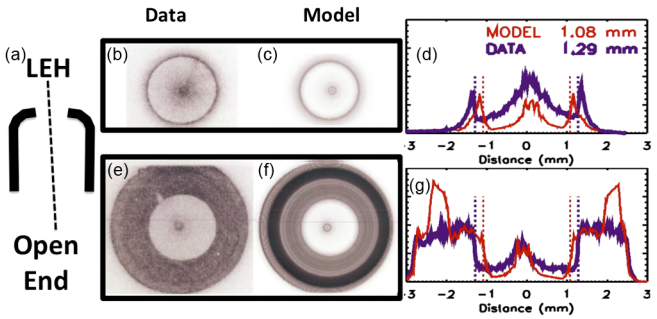

FIG. 5 (color online). (a) Schematic of ViewFactor target with dashed line showing observation axis for soft x-ray images. Images (b),(c), and (e),(f) are taken at 20 ns at an x-ray energy of 900 eV. Images are displayed with reverse color scale. (b) Data and (c) simulation looking into the LEH end. (d) Horizontal lineouts through the center of the data (blue, thick) and simulation (red, thin) images. (e) Data and (f) simulation looking into the open end and seeing the LEH at the far end. The very dark ring in simulation (f) is from the outer beams. The CH ball has collapsed to the bright, small object in the center of the LEH. (g) Horizontal lineouts through the center of the data (blue, thick) and simulation (red, thin) images. The simulation intensity has been multiplied by a single number to match the data in the lineouts in (g) at 1.5 mm. The vertical dashed lines in the lineouts (d) and (g) are the measured LEH radii, 1.29 mm for data and 1.08 mm for simulation.

17.5 ns, to within the 7% error bars of the Dante diagnostic, the multipliers are explained by the model's overprediction of the hohlraum emission directed at the capsule. This key conclusion highlights the need to focus on the physics of the hohlraum's conversion of laser light into x rays as opposed to the ablation model for the plastic capsule.

Time resolved views of the LEH from the upper pole for an ignition hohlraum are complicated by the glow from the opposite LEH. Using the ViewFactor platform, however, we are able to make unambiguous time-resolved measurements of the LEH size as there is no opposing LEH. Figure 5 shows an example of the data and modeled images from the 900 eV channel at 20 ns. The steep features in the plotted lineouts have the same diameter as seen from inside or outside the LEH. Comparing the model to the data at the four times (17, 18.5, 20, and 21.5 ns), shows that the model matches the weak time dependence of the measured LEH size but consistently underpredicts the LEH radius. The simulated LEH radius is ~84% of the measured LEH radius, meaning the area is ~70% of the measured area.

The ViewFactor experiments provide for the first time a direct measurement of the x-ray drive of an ignition hohlraum onto the capsule. The measured reduced drive compared to simulation identifies the hohlraum model as the source of the discrepancy in the slower than expected capsule implosion velocity, a discrepancy that has been compensated for in simulations with laser power multipliers. Additionally, the error in the calculated LEH closure is responsible for the serendipitous agreement between simulation and data when the radiation drive measurements through the LEH are compared.

Many aspects of the methodology used to simulate ignition hohlraums are now under study in an attempt to better reproduce the ViewFactor data. In particular, more attention is being paid to the low-density "bubble" of hot gold plasma that develops under the outer beam laser spots during the peak of the pulse between the cooler, higher-density wall and the helium fill. In this region where the bulk of the laser energy deposition occurs, the partitioning of energy between electrons and radiation has a significant influence on the capsule x-ray flux. Associated physics that may affect this process includes thermal transport (including nonlocality), nonlocal thermodynamic equilibrium kinetics, and hydrodynamic mixing at the unstable interface between the expanding gold plasma and the helium gas. In pursuit of a more accurate representation of the laser energy delivery to the hohlraum, an in-line energy transfer model which has transfer only in the overlapping parts of quads (instead of the entire beam spot) is in progress [20]. Finally, the open geometry of the ViewFactor target has provided a rich set of time-integrated and time-resolved image data, of which Fig. 5 is an example. Such data are well suited to either validate or eliminate the phenomena listed above and guide the process of improving the gas-filled ignition hohlraum model.

The authors would like to acknowledge the efforts of the NIF Operations, Laser Performance, Target Diagnostics, and Target Fabrication Teams. This work was performed under the auspices of the Lawrence Livermore National Security, LLC, (LLNS) under Contract No. DE-AC52-07NA27344.

*maclaren2@llnl.gov

[1] E. I. Moses, R. N. Boyd, B. A. Remington, C. J. Keane, and R. Al-Ayat, Phys. Plasmas **16**, 041006 (2009).
[2] J. D. Lindl, P. Amendt, R. L. Berger, S. Gail Glendinning, S. H. Glenzer, S. W. Haan, R. L. Kauffman, O. L. Landen, and L. J. Suter, Phys. Plasmas **11**, 339 (2004).
[3] S. W. Haan *et al.*, Phys. Plasmas **18**, 051001 (2011).
[4] D. G. Hicks *et al.*, Phys. Plasmas **19**, 122702 (2012).
[5] N. Meezan *et al.*, Phys. Plasmas **20**, 056311 (2013).
[6] O. S. Jones *et al.*, Phys. Plasmas **19**, 056315 (2012).
[7] W. Goldstein and R. Rosner, Technical Report No. LLNL-TR-570412, Lawrence Livermore National Laboratory, 2012.
[8] M. D. Rosen *et al.*, High Energy Density Phys. **7**, 180 (2011).
[9] http://www.prism-cs.com/Software/VisRad/VisRad.htm.
[10] P. Michel *et al.*, Phys. Plasmas **16**, 042702 (2009).
[11] J. Kline *et al.*, Rev. Sci. Instrum. **81**, 10E321 (2010).
[12] J. R. Kimbrough, P. M. Bell, D. K. Bradley, J. P. Holder, D. K. Kalantar, A. G. MacPhee, and S. Telford, Rev. Sci. Instrum. **81**, 10E530 (2010).
[13] J. Ze, R. L. Kauffman, J. D. Kilkenny, J. Wielwald, P. M. Bell, R. Hanks, J. Stewart, D. Dean, J. Bower, and R. Wallace, Rev. Sci. Instrum. **63**, 5124 (1992).
[14] J. D. Moody *et al.*, Nat. Phys. **8**, 344 (2012).
[15] G. B. Zimmerman and W. L. Kruer, Comments Plasma Phys. Control. Fusion **2**, 51 (1975).
[16] N. B. Meezan *et al.*, Phys. Plasmas **17**, 056304 (2010).
[17] H. Scott and S. Hansen, High Energy Density Phys. **6**, 39 (2010).
[18] R. P. J. Town *et al.*, Phys. Plasmas **18**, 056302 (2011).
[19] M. May *et al.*, AIP Conf. Proc. **730**, 61 (2004).
[20] M. Marinak and N. Meezan (private communication).